



## **HYDIN Variants Are a Common Cause of Primary Ciliary Dyskinesia in French Canadians**

To the Editor:

Primary ciliary dyskinesia (PCD) is a rare genetic disorder resulting in chronic sino-oto-pulmonary infections, bronchiectasis, and organ laterality defects (Online Mendelian Inheritance in Man #244400). Various PCD diagnostic tests are recommended per American Thoracic Society and European Respiratory Society clinical practice guidelines (1, 2), including nasal nitric oxide (nNO) measurement, ciliary ultrastructural analysis on transmission electron microscopy (TEM), ciliary beat pattern analysis with high-speed video microscopy, and genetic testing for PCD-related genes. However, no single diagnostic test detects all forms of PCD. In the past two decades, more than 50 PCD-related genes have been discovered (3), but most commercial genetic multigene panels analyze only a portion of these using next-generation sequencing (NGS) techniques.

Recently, a known PCD gene, *HYDIN* (HYDIN axonemal central pair apparatus protein; chromosome 16, NM\_001270974.2, Online Mendelian Inheritance in Man #608647), rarely associated with PCD and mostly in consanguineous individuals from the Faroe Islands (c.922A>T [p.Lys308Ter]; ClinVar identifier 39699), was implicated in 8% of suspected European PCD cases with normal organ arrangement (*situs solitus*) (4). Inherited in an autosomal-recessive pattern and encoding a ciliary protein in the central apparatus, *HYDIN* is a large gene (85 coding exons, 5,121 amino acids), with biallelic pathogenic variants causing PCD. The phenotypic characteristics are reported as *situs solitus*, normal results on TEM, and low nNO (5). Presence of the nearly identical pseudogene *HYDIN2* (HYDIN axonemal central pair apparatus protein 2; chromosome 1) complicates mutational analysis, as additional steps are necessary to ascertain the identified variants map on *HYDIN*. Hence, most commercial genetic panels do not include variant analysis of this large, complex, and seemingly rare PCD gene.

Supported by National Center for Advancing Translational Sciences (NCATS) grant U54HL096458 (M.R.K., M.W.L., M.A.Z., S.D.D., and A.J.S.) and National Heart, Lung, and Blood Institute grant R01HL071798 (M.R.K. and M.A.Z.). The Genetic Disorders of Mucociliary Clearance Consortium (U54HL096458) is part of the NCATS Rare Diseases Clinical Research Network (RDCRN) and supported by the RDCRN Data Management and Coordinating Center (National Institutes of Health grant U2CTR002818). RDCRN is an initiative of the Office of Rare Diseases Research funded through a collaboration between NCATS and the National Heart, Lung, and Blood Institute. The Yale Center for Mendelian Genomics is funded by National Human Genome Research Institute grant UM1HG006504. The GSP Coordinating Center (supported by NCATS grant U24 HG008956) contributed to cross-program scientific initiatives and provided logistical and general study coordination. The content is solely the responsibility of the authors and does not necessarily represent the official views of the National Institutes of Health.

**Author Contributions:** A.J.S., G.S., D.D., L.B., M.W.L., S.D.D., M.R.K., and M.A.Z. all created the research protocol, assisted in data and sample collection, and contributed to writing the manuscript. M.A.Z., F.L.-G., and S.M. performed whole-exome genetic sequencing and analysis. All authors approve of this manuscript in its current form. A.J.S. is the guarantor of the paper, taking responsibility for the integrity of the work as a whole, from inception to published article.

The PCD clinic at McGill University Health Centre (MUHC; Montreal, Quebec, Canada) is the provincial referral site for suspected PCD cases, following 104 patients with PCD (84 families), with 76 patients (63 families) who are definitively diagnosed through TEM defects and/or molecular genetic testing. The remaining 28 patients with probable PCD (21 families) display strong PCD clinical phenotypes but are “unsolved,” with normal or inconclusive TEM findings and nondiagnostic commercial genetic panels testing 30–36 PCD-related genes (not including *HYDIN*). In each family, cystic fibrosis and immunodeficiency test results are negative, and most have nNO < 77 nl/min (6). We hypothesized that *HYDIN* played a significant role in these unsolved cases.

### **Methods**

Human studies with informed consent were completed per approved Institutional Review Board protocols. Unsolved PCD cases from 2015 to 2021 were investigated through two distinct protocols as they were available: 1) from 2015 to 2018 (MUHC Research Ethics Board #14-138-PED), research whole-exome sequencing and analysis (WES), as described previously (7, 8), through the Genetic Disorders of Mucociliary Clearance Consortium, and 2) from 2019 to 2021 (MUHC Research Ethics Board #2021-7474), 43 PCD multigene commercial panels through Blueprint Genetics, analyzing 62 of 85 *HYDIN* exons using NGS (9). In cases investigated using WES, allele-specific PCR and Sanger sequencing were used to ascertain that identified variants were indeed residing in *HYDIN* and not in *HYDIN2*, but we did not perform copy number variant analysis in samples evaluated using WES. In cases analyzed with NGS multigene panels, bidirectional Sanger sequencing or digital polymerase chain reaction methods were used to orthogonally confirm variants that did not meet rigorous internal sequencing quality score thresholds and other proprietary laboratory criteria with Blueprint Genetics (<https://blueprintgenetics.com/pseudogene>). NGS analysis also confirmed copy number variants if they were <10 exons (heterozygous) or <3 exons (homozygous or hemizygous) in size or had not been confirmed at least three times previously in Blueprint’s laboratory. We did not perform high-speed video microscopy analysis or ciliary protein immunofluorescence staining through any of these protocols.

### **Results**

In this single-center analysis, the most common PCD-related genes are *DNAH5* (dynein axonemal heavy chain 5;  $n = 11$  families [15.9%]), *DNAH11* (dynein axonemal heavy chain 11;  $n = 8$  families [11.6%]), *CCNO* (cyclin O;  $n = 4$  families [5.8%]), and *RSPH1* (radial spoke head component 1;  $n = 4$  families [5.8%]). Testing of our 21 unsolved PCD families revealed 6 additional families (11 cases, 36% male, median age 16.1 yr [range, 1–31 yr]) harboring two pathogenic or likely pathogenic *HYDIN* variants, confirming PCD. Both *HYDIN* variants were in *trans* where segregation studies were performed (Table 1). Five *HYDIN* families had normal TEM findings, with one additional family having inadequate or inconclusive TEM findings. Figure 1 two additional families carried only one pathogenic or likely pathogenic *HYDIN* variant, though one of these (M15, family 7) also had a variant of uncertain significance on an extended splice-acceptor site. None of these *HYDIN* variants is previously published in human cases of PCD, and specific variant details, including American College

**Table 1.** Genotype and phenotype characteristics of primary ciliary dyskinesia cases due to variants in *HYD1N* axonemal central pair apparatus protein among French Canadians in Quebec\*

ID, Fam	Age at Dx (y)	Gene Test	Variants (Base, Change, Protein Change, Zygosity, Inheritance, Variant Classification)	TEM	nNO (n/l/min) <sup>†</sup>	NRD	Year-Round Rhinitis <sup>‡</sup>	Sinusitis	Year-Round Wet Cough <sup>‡</sup>	Bronchiectasis on CT	OM	FEV <sub>1</sub> % Predicted	Sputum	Other
M03, fam 1 <sup>§</sup>	22	WES	c.5037 + 3A>G, p.?, het, mat, likely path c.6530A>C, p.(Gln2177Pro), het, pat, likely path	Normal	5	Y	Y	Y (P)	Y	ND	N	74	<i>P. multocida</i> , <i>S. aureus</i> , <i>H. influenzae</i>	
M07, fam 1 <sup>§</sup>	17	WES	c.5037 + 3A>G, p.?, het, mat, likely path c.6530A>C, p.(Gln2177Pro), het, pat, likely path	Normal	35, 31	N	N	Y (P)	Y	RML, ling, LLL	N	49	<i>P. multocida</i> , <i>S. aureus</i> , <i>H. influenzae</i>	Thoracic scoliosis 40°
M08, fam 2 <sup>§</sup>	13	WES	c.10426C>T, p.(Arg3476*), hom, na, path	Inadequate	33, 75	Y	N	N	Y	RML, LLL	N	78	<i>P. aeruginosa</i> , <i>S. aureus</i> , <i>H. influenzae</i>	Lumbar scoliosis 52°
M10, fam 2 <sup>§</sup>	15	WES	c.10426C>T, p.(Arg3476*), hom, na, path	Normal	5, 15	Y	Y	Y (P)	Y	No	Y	99	<i>S. aureus</i> , <i>H. influenzae</i> , <i>S. pneumoniae</i>	
M18, fam 3	17	WES	c.10426C>T, p.(Arg3476*), het, pat, path c.2979, 2995del, p.(Ser934Gfs*5), het, mat, likely path	Normal	TY	Y	Y	N	Y	ND	Y	TY	<i>M. catarrhalis</i>	PSP, intestinal malrotation
M91, fam 4 <sup>§</sup>	6	BPG	c.10426C>T, p.(Arg3476*), het, mat, likely path c.9352G>C, p.(Val3118Leu), het, mat, likely path	ND	22, 20	Y	Y	N	Y	ND	Y	108	<i>H. influenzae</i>	Thoracic scoliosis (mild), pectus excavatum
M93, fam 5 <sup>§</sup>	27	BPG	c.10426C>T, p.(Arg3476*), het, mat, path c.6427G>T, p.(Gly2143*), het, pat, path	Inadequate	26	N	Y	Y (P)	Y	RML, ling, RLL, LLL	Y	56	<i>P. aeruginosa</i> , <i>E. coli</i>	
M92, fam 5 <sup>§</sup>	31	BPG	c.10426C>T, p.(Arg3476*), het, mat, path c.6427G>T, p.(Gly2143*), het, pat, path	Inconclusive	ND	Unknown	Y	Y	Y	RML, RLL, LLL	Y	75	<i>P. aeruginosa</i> , <i>H. influenzae</i>	Infertility
M101, fam 6 <sup>  </sup>	14	BPG	c.10426C>T, p.(Arg3476*), hom, na, path	Normal	11, 17	N	Y	Y	Y	RML	Y	62	<i>S. aureus</i> , <i>H. influenzae</i>	Thoracolumbar scoliosis 15°
M107, fam 6 <sup>   </sup>	14	BPG	c.10426C>T, p.(Arg3476*), hom, na, path	ND	17	N	Y	Unknown	Y	RML	Y	89	<i>OP flora</i>	
M15, fam 7	7	WES	c.7594G>T, p.(Glu2532*), het, na, likely path c.3786-2dup**, het, na, VUS	Normal	10, 5	Y	Y	N	Y	ND	Y	94	<i>S. aureus</i> , <i>H. influenzae</i> , <i>E. cloacae</i> , <i>M. catarrhalis</i>	Infertility
M80, fam 8	49	BPG	c.9352G>C, p.(Val3118Leu) <sup>††</sup> , het, na, likely path	Normal	54, 36	Unknown	Y	Y	Y	RML, ling	Y	72	<i>P. aeruginosa</i>	

**Definition of abbreviations:** BPG = Blueprint Genetics 43-gene next-generation sequencing primary ciliary dyskinesia panel (9); CT = computed tomography; Dx = diagnosis; *E. cloacae* = enterobacter cloacae; *E. coli* = *Escherichia coli*; fam = family; FEV<sub>1</sub> = forced expiratory volume in 1 second by Global Lung Initiative standards; *H. influenzae* = *Haemophilus influenzae*; het = heterozygous; hom = homozygous; ID = identifier; ling = lingula; LLL = left lower lobe; *M. catarrhalis* = *Moraxella catarrhalis*; mat = maternal; N = no; na = not available; ND = not done; nNO = nasal nitric oxide (with repeated measures presented for some participants); NRD = neonatal respiratory distress at term birth; OM = recurrent otitis media; OP = oropharyngeal; P = nasal polyposis; pat = paternal; path = pathogenic; p. = protein change unknown; *P. aeruginosa* = *Pseudomonas aeruginosa*; *P. multocida* = *Pasteurella multocida*; PSP = polysplenia; RLL = right middle lobe; RML = right middle lobe; *S. aureus* = *Staphylococcus aureus*; *S. pneumoniae* = *Streptococcus pneumoniae*; TEM = transmission electron microscopy; TY = too young to perform; VUS = variant of uncertain significance; WES = whole-exome sequencing; Y = yes.  
 \*All participants except for families 5 and 7 had nondiagnostic results on 30–36 multigene next generation sequencing panels via Invitae (not including *HYD1N*; https://www.invitae.com/en/physician/tests/0410) before enrollment in this protocol. Family 5 only had clinical genetic testing via BPG, while family 7 only underwent WES analysis.  
 †nNO measurements were performed on two separate visits for most participants, but there was only one visit for three participants.  
 ‡Symptom onset in early infancy.  
 §Sibiling pair.  
 ||First cousin pair.  
 |||Known parental consanguinity (double first cousins).  
 \*\*Currently, this ultrarare variant in one population database (Genome Aggregation Database [https://gnomad.broadinstitute.org]) is considered a VUS, as no functional studies are available for this splice extended site variant.  
 ††Identical likely pathogenic variant as in family 4, but no known common relatives. No second *HYD1N* variant was found on commercial genetic testing that profiles only 62 of the 85 coding exons.

Table 2. Characteristics of specific HYDIN axonemal central pair apparatus protein variants

HYDIN Variant*	Protein Change	rsID	Variant Type	ACMG-AMP Guided Pathogenicity (15)	gnomAD Variant Name	gnomAD Frequency <sup>†</sup>	SpliceAI Score <sup>‡</sup>	Conservation Score (CADD) <sup>§</sup>	Conservation Score (REVEL) <sup>  </sup>	Variant Details
c.2979_2995del	p.(Ser993Argfs*5)	—	Frameshift	Likely pathogenic	—	Absent	0.18 (donor loss)	N/A	N/A	Deletes 17 bp in exon 20, generating a frameshift with premature stop codon at position 5 in new reading frame.
c.3786-2dup	p.?	rs1567959976	Splice acceptor	Uncertain significance	16-71025300-C-CT	0.000008	0.53 (acceptor loss)	22.7	N/A	Duplicates a nucleotide within a canonical splice acceptor, predicted to only slightly weaken the splice acceptor of intron 24.
c.5037+3A>G	p.?	rs556958197	Intron variant	Likely pathogenic	16-70974170-T-C	0.000007	0.72 (donor loss)	13.06	N/A	Nucleotide substitution weakens splice donor of intron 33 and is predicted to disrupt splicing.
c.6427G>T	p.(Gly2143*)	—	Nonsense	Pathogenic	—	Absent	0	32	N/A	Generates a premature stop codon in exon 41 and is predicted to lead to loss of normal protein function through protein truncation (2,142 of 5,121 aa) or nonsense-mediated mRNA decay.
c.6530A>C	p.(Gln2177Pro)	—	Missense/splice donor	Likely pathogenic	—	Absent	0.62 (donor loss)	25.3	0.194	Substitution of the penultimate nucleotide of exon 41 is predicted to weaken the splice donor of intron 41 and may disrupt splicing.
c.7594G>T	p.(Glu2532*)	—	Nonsense	Likely pathogenic	—	Absent	0	41	N/A	Generates a premature stop codon in exon 46 and is predicted to lead to loss of normal protein function through protein truncation or nonsense-mediated mRNA decay.
c.9352G>C <sup>  </sup>	p.(Val3118Leu)	rs545412163	Missense	Likely pathogenic	16-709266329-C-G	0.000046	0	23.1	0.106	Amino acid change according to <i>in silico</i> prediction tools on protein structure and function is predicted to be damaging per SIFT, disease causing per MutationTaster, and possibly damaging per PolyPhen. Likely pathogenic classification per Blueprint Genetics.
c.10426C>T	p.(Arg3476*)	rs780790869	Nonsense	Pathogenic	16-70913331-G-A	0.000018	0.05 (donor gain)	39	N/A	Generates a premature stop codon in exon 62 and is predicted to lead to loss of normal protein function through protein truncation (3,475 of 5,121 aa) or nonsense-mediated mRNA decay.

*Definition of abbreviations:* aa = amino acids; ACMG = American College of Medical Genetics and Genomics; AMP = Association for Molecular Pathology; CADD = Combined Annotation Dependent Deletion; gnomAD = Genome Aggregation Database; HYDIN = HYDIN axonemal central pair apparatus protein; mRNA = messenger ribonucleic acid; N/A = not applicable; p. ? = protein change unknown; REVEL = Rare Exome Variant Ensemble Learner; rsID = Reference Single Nucleotide Polymorphism Cluster ID; SIFT = Sorting Intolerant from Tolerant.

\*All variant nomenclatures correspond to transcript NM\_001270974.2.

<sup>†</sup>gnomAD (version 2) except for c.5037+3A>G variant, which is found in gnomAD (version 3).

<sup>‡</sup>SpliceAI scores range from 0 to 1, with values >0.5 suggesting higher likelihood that a variant is splice altering (<https://github.com/Illumina/SpliceAI>).

<sup>§</sup>CADD scores range from 1 to 99, with values >20 suggesting higher likelihood that a variant is deleterious (<https://cadd.gs.washington.edu>).

<sup>||</sup>REVEL scores range from 0 to 1, with values >0.5 suggesting higher likelihood that a missense variant is disease causing (<https://sites.google.com/site/revelgenomics/>).

<sup>¶</sup>This missense variant appears to be disease causing on the basis of the *in silico* prediction tools, segregation analysis, and classification by Blueprint Genetics. However, the possibility that this variant is in *cis* with another pathogenic variant in the region of the gene not ascertained using current methodologies (such as large deletions or deep intronic variants) cannot be ruled out.

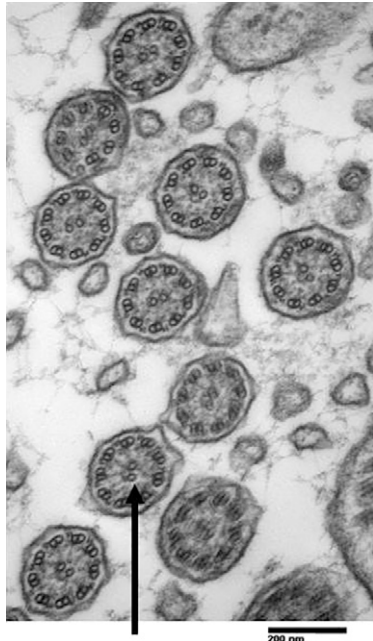


**Figure 1.** Transmission electron microscopy in a participant with *HYDIN*-related disease. Ciliary cross-sections from participant M101 (*HYDIN* c.10426C>T, p.[Arg3476\*], homozygous) showing normal ultrastructure with 9 + 2 arrangement of the outer microtubule doublets and central apparatus plus visible outer and inner dynein arms; 80,000 $\times$  magnification. Nondiagnostic electron microscopy changes may be seen in *HYDIN*-associated cases, including shrunken central pairs and occasional translocations of peripheral doublets to the central pair area (not pictured here). Suggestion of an absent C2b projection from the central apparatus can also be identified (surrounding white spaces and clearly visible radial spoke heads, black arrow). Definitive absence of the C2b projection requires advanced imaging techniques, including image averaging microscopy and computed tomography of affected cilia (5). *HYDIN*=HYDIN axonemal central pair apparatus protein.

of Medical Genetics and Genomics pathogenicity classifications, can be found in Table 2.

Interestingly, five families (nine cases) harbored a common *HYDIN* variant in a homozygous or compound heterozygous state. This nonsense pathogenic variant (c.10426C>T, p.[Arg3476\*]), presumed to generate premature translation termination in exon 62, is predicted to cause loss of normal protein function, either through protein truncation (3,475 of 5,121 amino acids) or nonsense-mediated messenger ribonucleic acid decay. This ultrarare variant is not in ClinVar or the Human Gene Mutation Database, but five heterozygotes (no homozygotes) appear in the Genome Aggregation Database, which covers >15,000 genomes. Each participant with the c.10426C>T variant was White and of French Canadian ancestry, with both sets of grandparents born in Quebec and known parental consanguinity in one patient.

All subjects with *HYDIN* had normal organ arrangement except for one (M90, polysplenia and intestinal malrotation, unclear if PCD related or incidental), and all displayed classic PCD phenotypes with low nNO (median 24 nl/min; range, 5–75 nl/min). Four cases had scoliosis, which has not been associated with *HYDIN* (Table 1). Median forced expiratory volume in 1 second was 77% predicted

(range, 49–108%), six cases (55%) had bronchiectasis at diagnosis, and four cases (36%) had *Pseudomonas aeruginosa* in sputum cultures.

## Discussion

Pathogenic variants in *HYDIN* aided diagnosis in 6 of 21 (28.5%) families with previously unsolved PCD. Thus, pathogenic variants in *HYDIN* are responsible for a large percentage of PCD in Quebec, accounting for 6 of 69 (8.7%) families with definitively diagnosed PCD in this provincial clinic. This makes *HYDIN* the third most prevalent PCD gene (after *DNAH5* and *DNAH11*) in our Quebec cohort. The high proportion of *HYDIN*-related variants in our cohort may be related to our enrollment of mainly cases with unsolved PCD with low nNO values (which are associated with *HYDIN* but less so with other PCD genes known to result in nondiagnostic TEM images) (10). However, we speculate that the prevalence of such variants may be even greater once the remaining 23 *HYDIN* exons are analyzed in our commercially unsolved (NGS) PCD cases. Although this high prevalence may be due to a possible founder variant at c.10426C>T, other *HYDIN* variants were observed, meaning that a founder effect alone is not responsible for the high burden of pathogenic variants in *HYDIN* among French Canadians in Quebec.

The median diagnostic age for our subjects with *HYDIN* is 16 years, which is older than the median diagnostic age of 6 years reported in the PCD literature (11). This delay likely reflects decreased clinical consideration of PCD in patients lacking organ laterality defects or TEM ultrastructural defects. Yet most of these *HYDIN*-related patients presented as newborns with respiratory distress and displayed other classic PCD symptoms of year-round wet cough and year-round rhinosinusitis from infancy (12). As knowledge of the classic PCD phenotype increases, patients such as these will hopefully be diagnosed at earlier ages, allowing them to start routine PCD therapies.

Initially discovered as a cause of human PCD in 2012, *HYDIN* encodes a protein residing in the c2b projection of the central apparatus. Before this, *HYDIN* variants in the murine ortholog *hy3* (hydrocephalus 3) were studied as a hydrocephalus model because of effects on motile, ependymal cilia (13). Unfortunately, early postnatal death of *hy3* murine models precluded study of a PCD respiratory phenotype, but a complete lack of organ laterality defects was noted (14). Before 2020, <25 overall families with *HYDIN* causing PCD were published, and because of the complex genetic and ultrastructural analyses required, *HYDIN* assessment was relegated mainly to research laboratories, without incorporation into clinical PCD testing. With abnormal, rotational beat patterns on high-speed video microscopy, more *HYDIN*-related cases were likely detected at some European PCD centers performing ciliary beat pattern analysis on high-speed video microscopy, but these cases were largely unconfirmed through genetic testing. In 2020, absent immunofluorescent antibody staining for *SPEF2* (sperm flagellar 2), a central apparatus chaperone protein in the c1b projection assisting with *HYDIN* protein colocalization in the c2b projection, suggested that *HYDIN* variants were responsible for a larger proportion of PCD in Europe than initially considered (4). Our data support this suspicion of *HYDIN* variants' causing a larger number of human PCD cases than previously believed, and we report approximately the same prevalence in our population as in the recent European cohort. Unfortunately, we were not able to perform similar *SPEF2*



immunofluorescent analysis in this cohort, though this testing may have helped confirm additional HYDIN cases unsolved via genetic testing (Table 1, cases M15 and M80).

As *HYDIN* is one of the largest PCD-related genes, the potential for genetic lesions is accordingly increased, and it is possible that *HYDIN* accounts for a significant percentage of PCD across North America. Recent analysis of the PCD Foundation Clinical and Research Center Network reveals that the majority of sites use commercial genetic panels that do not include *HYDIN* analysis. It is not clear if our increased *HYDIN* prevalence will be observed in populations outside Quebec, but it is tempting to speculate a widespread higher prevalence given the allelic heterogeneity already observed in this cohort. Thus, transitioning to commercial panels that analyze *HYDIN* seems critical to accurately diagnose patients with PCD, notably those with situs solitus, normal TEM findings, and low nNO. ■

**Author disclosures** are available with the text of this letter at [www.atsjournals.org](http://www.atsjournals.org).

**Acknowledgment:** The authors thank the study patients and families at McGill University for their participation. The authors thank the investigators and coordinators of the Genetic Disorders of Mucociliary Clearance Consortium, which is part of the Rare Disease Clinical Research Network; Dr. Jaclyn Stonebraker and Elizabeth Schecterman for technical assistance and Dr. Hong Dang for bioinformatics assistance; and Kelli Sullivan and Nicole Capps for help with specimen accrual and coordination. The authors thank Dr. Weilai Dong of the Yale Center for Mendelian Genomics for providing support with bioinformatics and analysis of WES. The authors also thank Blueprint Genetics for assistance in drafting text describing their orthogonal variant confirmation policy and Dr. Jean-Baptiste Rivière of the MUHC Research Institute for his support with variant classification and frequencies.

Adam J. Shapiro, M.D.\*  
Guillaume Sillon, M.Sc., C.G.A.C.  
Daniela D'Agostino, M.D., M.Sc., F.R.C.P.C.  
Laurence Baret, M.A., M.Sc., C.C.G.C., C.G.C.  
McGill University  
Montreal, Quebec, Canada

Francesc López-Giráldez, Ph.D., B.S.  
Shrikant Mane, Ph.D.  
Yale University  
New Haven, Connecticut

Margaret W. Leigh, M.D.  
Stephanie D. Davis, M.D.  
Michael R. Knowles, M.D.  
Maimoona A. Zariwala, Ph.D.  
University of North Carolina  
Chapel Hill, North Carolina

ORCID ID: 0000-0001-6066-6750 (A.J.S.).

\*Corresponding author (e-mail: [adam.shapiro@muhc.mcgill.ca](mailto:adam.shapiro@muhc.mcgill.ca)).

## References

- Shapiro AJ, Davis SD, Polineni D, Manion M, Rosenfeld M, Dell SD, et al.; American Thoracic Society Assembly on Pediatrics. Diagnosis of primary ciliary dyskinesia: an official American Thoracic Society clinical practice guideline. *Am J Respir Crit Care Med* 2018;197:e24–e39.
- Lucas JS, Barbato A, Collins SA, Goutaki M, Behan L, Caudri D, et al. European Respiratory Society guidelines for the diagnosis of primary ciliary dyskinesia. *Eur Respir J* 2017;49:1601090.
- Zariwala MA, Knowles MR, Leigh MW. Primary ciliary dyskinesia. In: Adam MP, Ardinger HH, Pagon RA, Wallace SE, Bean LJH, Gripp KW, et al., editors. *GeneReviews*<sup>®</sup>. Seattle, WA: University of Washington, Seattle; 2021.
- Cindrić S, Dougherty GW, Olbrich H, Hjejij R, Loges NT, Amirav I, et al. *SPEF2*- and *HYDIN*-mutant cilia lack the central pair-associated protein *SPEF2*, aiding primary ciliary dyskinesia diagnostics. *Am J Respir Cell Mol Biol* 2020;62:382–396.
- Olbrich H, Schmidts M, Werner C, Onoufriadis A, Loges NT, Raidt J, et al.; UK10K Consortium. Recessive *HYDIN* mutations cause primary ciliary dyskinesia without randomization of left-right body asymmetry. *Am J Hum Genet* 2012;91:672–684.
- Shapiro AJ, Dell SD, Gaston B, O'Connor M, Marozkina N, Manion M, et al. Nasal nitric oxide measurement in primary ciliary dyskinesia: a technical paper on standardized testing protocols. *Ann Am Thorac Soc* 2020;17:e1–e12.
- Smith AJ, Bustamante-Marin XM, Yin W, Sears PR, Herring LE, Dicheva NN, et al. The role of SPAG1 in the assembly of axonemal dyneins in human airway epithelia. *J Cell Sci* 2022;135:jcs259512.
- Van der Auwera GA, Carneiro MO, Hartl C, Poplin R, Del Angel G, Levy-Moonshine A, et al. From FastQ data to high confidence variant calls: the Genome Analysis Toolkit best practices pipeline. *Curr Protoc Bioinform* 2013;43:11.10.11–11.10.33.
- Blueprint Genetics. Primary ciliary dyskinesia panel. Seattle, WA: Blueprint Genetics; 2022 [accessed 2022 Jul 30]. Available from: <https://blueprintgenetics.com/tests/panels/nephrology/primary-ciliary-dyskinesia-panel/>.
- Raidt J, Krenz H, Tebbe J, Große-Onnebrink J, Olbrich H, Loges NT, et al. Limitations of nasal nitric oxide measurement for diagnosis of primary ciliary dyskinesia with normal ultrastructure. *Ann Am Thorac Soc* 2022;19:1275–1284.
- Kuehni CE, Frischer T, Strippoli MP, Maurer E, Bush A, Nielsen KG, et al.; ERS Task Force on Primary Ciliary Dyskinesia in Children. Factors influencing age at diagnosis of primary ciliary dyskinesia in European children. *Eur Respir J* 2010;36:1248–1258.
- Leigh MW, Ferkol TW, Davis SD, Lee HS, Rosenfeld M, Dell SD, et al. Clinical features and associated likelihood of primary ciliary dyskinesia in children and adolescents. *Ann Am Thorac Soc* 2016;13:1305–1313.
- Davy BE, Robinson ML. Congenital hydrocephalus in *hy3* mice is caused by a frameshift mutation in *Hydin*, a large novel gene. *Hum Mol Genet* 2003;12:1163–1170.
- Lechtreck KF, Delmotte P, Robinson ML, Sanderson MJ, Witman GB. Mutations in *Hydin* impair ciliary motility in mice. *J Cell Biol* 2008;180:633–643.
- Richards S, Aziz N, Bale S, Bick D, Das S, Gastier-Foster J, et al. Standards and guidelines for the interpretation of sequence variants: a joint consensus recommendation of the American College of Medical Genetics and Genomics and the Association for Molecular Pathology. *Genet Med* 2015;17:405–424.

Copyright © 2023 by the American Thoracic Society